Effect of Overlapping Resonances in Final States*†

P. K. SRIVASTAVA†
The Enrico Fermi Institute for Nuclear Studies and the Department of Physics, The University of Chicago, Chicago, Illinois
(Received 31 December 1962)

By introducing an $N\theta$ scattering resonance, the $V\theta$, $N\theta\theta$ sector of the Lee model provides a calculable model for reaction processes leading to a three-particle final state where two overlapping resonances can occur. The $V\theta$ scattering and reaction cross sections calculated are found to be free of any bump in the energy range corresponding to overlap of the two final $N\theta$ resonances. The $V\theta$ scattering amplitude is analytically continued to higher Riemann sheets, and the singularity analogous to that conjectured by Peierls to be the cause of higher resonances in the pion-nucleon system has been shown to lie on a Riemann sheet far from the physical domain. These results cast considerable doubt on the validity of this proposed mechanism for the production of higher resonances.

1. INTRODUCTION

IN the study of the reactions of the strongly interacting particles, we find that most of the cross sections are dominated by bumps in definite angular momentum and parity states. This dominance of the cross sections by isolated resonances is in itself a considerable simplification of the most general situation, as it allows us to describe the situations by a finite number of parameters. The number of parameters can be further reduced if some of these resonances conspire to produce some of the others. This hope has motivated several authors[1,2] to propose models for the second pion-nucleon resonance. One of these, due to Peierls,[1] is the subject matter of this communication. Peierls has made an attempt to explain the higher pion-nucleon resonance as a dynamical consequence of the lowest pion-nucleon resonance, the well-known (3,3) isobar. His model consists of taking the isobar seriously as a particle; thus, he can consider the amplitude of the pion-isobar scattering as an amplitude relevant in the final-state scattering effect in the process $\pi N \rightarrow \pi\pi N$. He then looks for the singularities of the $\pi N^* - \pi N^*$ amplitude [N^* denotes the (3,3) resonance] and finds that the Born approximation singularity in the crossed-channel falls in the region of the physical energies, and numerically is in the correct position to be considered as a likely candidate for the second pion-nucleon resonance. This singularity is necessarily below the pion-isobar threshold in the case of the isobar being stable. The question now arises whether this singularity (of the phantom πN^* amplitude) will show up in any physical amplitude or not. At this juncture Peierls conjectures that it shows up in all the coupled channels. Tuan[3] follows up this lead and predicts a number of bumps in the $\bar{K}N$ channel based on taking Y^* ($\pi\Lambda$ resonance) as the causative agent.

We can visualize the content of the Peierls mechanism in a straightforward fashion by looking at the Dalitz plot of the $N\pi\pi$ state. Certainly there is an enhancement of the reaction along the bands where one or the other of the $N\pi$ pairs is in resonance. When the total energy is equal to twice the energy of the resonance, then these two bands will cross in the physical region of the Dalitz plot, and it is unlikely that this crossing region, which is necessarily small, can dominate the total cross section. What is required for the Peierls mechanism to be applicable is a general enhancement of the reaction over the whole of the Dalitz plot. This fact has already been emphasized by Tuan. There is no physically obvious way in which such an enhancement can be conceived. We find it worth while to re-examine the model taking unitarity into account. Goebel[4] has looked into the problems associated with treating the unstable particles on the same footing as the stable ones in this particular context, and has come to the conclusion that the particular singularity considered by Peierls is present in the $\pi N - \pi N$ amplitude at the same energy; however, it is not on the second sheet, but on a higher Riemann sheet of the energy plane.

In this paper, we try to carry the Peierls mechanism a step forward by calculating the effect of unitarity exactly for a particular model. It should be noticed that the pion-isobar system is, in fact, a 3-particle system, and, hence, any attempt to introduce unitarity is thwarted by the complication of the complete five-point functions. We simplify the problem to the barest essentials by eliminating all the extraneous states and all the momentum transfer variables. This we achieve by working in a generalized Lee model.[5] The model used describes the interaction of three static fermions V, V_1, and N with a light boson θ via the interaction $V \rightarrow N+\theta$ and $V_1 \rightarrow N+\theta$. All the particles are assumed to have no antiparticles; also all the interactions are assumed to be in s states. The physical situation discussed by Peierls is then simulated in essence by considering V_1 as unstable. The particles V and N in

* A thesis submitted to the Department of Physics, the University of Chicago, in partial fulfillment of the requirements for the Ph.D. degree.

† This work was supported in part by the U. S. Atomic Energy Commission at the University of Chicago.

‡ Present address: Indiana University, Bloomington, Indiana.

[1] R. F. Peierls, Phys. Rev. Letters **6**, 641 (1961).

[2] L. F. Cook and B. W. Lee, Phys. Rev. **127**, 297 (1962).

[3] S. F. Tuan, Phys. Rev. **125**, 1761 (1962).

[4] C. F. Goebel (to be published).

[5] P. K. Srivastava, Phys. Rev. **128**, 2906 (1962).

the model correspond to the nucleon and the V_1 corresponds to the isobar. Graphs typical of the Peierls model are present in the $V\theta$ scattering. Thus, important inferences can be drawn from an exact solution of the $V\theta$ scattering. Such a solution has already been obtained by Amado[6] in the usual Lee model, and shown to be unitary. We have carried out a numerical calculation using a modification of Amado's solution, modified to take into account an unstable V_1 particle. The calculations were carried out for a wide range of parameters. No bumps were found either in the elastic or the inelastic $V\theta$ cross sections. The $V\theta$ scattering amplitude was analytically continued as a function of the total energy variable, across the three-particle branch cut, and a complex cut in the second sheet; a singularity was found near the position conjuctured by Peierls but on a sheet far removed from the physical sheet. In Sec. 3 of this paper, an attempt is made to correlate the singularities discussed in Sec. 2 with those of a model in which both the V particles are stable.

2. $V\theta$ SCATTERING IN THE GENERALIZED LEE MODEL

The particular generalization of the Lee model[5] with which we are concerned has two V particles, instead of one as in the usual Lee model.[7] When both the V particles are stable, we can easily write down the Hamiltonian of the system and solve the appropriate Schrödinger equations to obtain the wave functions of the physical V states. Also the model can be described in a completely renormalized form. In the present case, where we want to deal with the situation when one of the V particles is in the $N\theta$ continuum, the renormalization program can not be carried out explicitly; therefore, we find it profitable to describe the unstable V particle in terms of (C.D.D.)[8] pole parameters instead of the usual mass and coupling constant. In the case under consideration, the stable $|V\rangle$ state and the $|N\theta^+\rangle$ scattering states themselves form a complete set of states spanning this particular sector of the Lee model. (The states in the Lee model split up into these sectors due to the stringent selection rules imposed by the absence of antiparticles and the restricted interaction $V \rightleftarrows N+\theta$. Thus, there are only two types of states in each sector, e.g., V and $N\theta$, $V\theta$ and $N\theta\theta$, etc. This splitting up of the states into finite sectors is one of the reasons which make the Lee model soluble.) When we introduce these states in the decomposition of the scattering amplitude for the $N\theta$ system, we get the following dispersion relation

$$M(\omega)=-\frac{g^2}{\omega}+\frac{1}{\pi}\int_\mu^\infty \frac{k'u^2(\omega')|M(\omega')|^2d\omega'}{4\pi(\omega'-\omega-i\epsilon)}, \quad (2.1)$$

where $u^2(\omega)$ is the cutoff function introduced to obtain convergence in the integrals. The mass of the V particle has been chosen equal to that of the N particle, and for convenience the zero of energy is also chosen to be the mass of the N particle.[9] The mass of the θ particle is taken to be μ and it obeys a relativistic energy momentum relation. The equation obtained for $M(\omega)$ is a Low-type equation which has a solution

$$M(\omega)=-\frac{g^2}{\omega}\frac{1}{1-\beta(\omega)}, \quad (2.2)$$

where

$$1-\beta(\omega)=1+\frac{g^2}{4\pi^2}\omega\int_\mu^\infty \frac{k'u^2(\omega')d\omega'}{\omega'^2(\omega'-\omega-i\epsilon)} \quad (2.3)$$

and

$$k=(\omega^2-\mu^2)^{1/2}. \quad (2.4)$$

The integral equation (2.1) only defines the residue of the function $M(\omega)$ at the pole at $\omega=0$ and the discontinuity across the cut from $\omega=\mu$ to $\omega=\infty$. This information is insufficient to define the function $M(\omega)$ completely, and gives one the freedom to modify the function $1-\beta(\omega)$ by adding a number of C.D.D.[8] poles. In our case, we modify the function by adding $-A\omega/(\omega-\omega_0)$, where A and ω_0 are real constants.

$$1-\beta(\omega)=1+\frac{g^2}{4\pi^2}\omega\int_\mu^\infty \frac{k'u^2(\omega')d\omega'}{\omega'^2(\omega'-\omega-i\epsilon)}-\frac{A\omega}{\omega-\omega_0}. \quad (2.5)$$

The parameters have to be so restricted that $1-\beta(\mu)>0$. In that case, $1-\beta(\omega)$ does not have any zeros in the cut ω plane. There are, however, zeros in the II sheet which for sufficiently large ω lie at complex conjugate points m and m^*. This is precisely the form of the $N\theta$ amplitude in the presence of two V particles as obtained by the Hamiltonian method when one of the V particles is unstable. When ω_0 is varied so as to violate the condition $1-\beta(\mu)>0$ an extra pole is obtained in $M(\omega)$ and we get the $N\theta$ scattering amplitude applicable to the Lee model with two stable V particles. With these comments on the $N\theta$ scattering, we turn our attention to the $V\theta$ scattering.

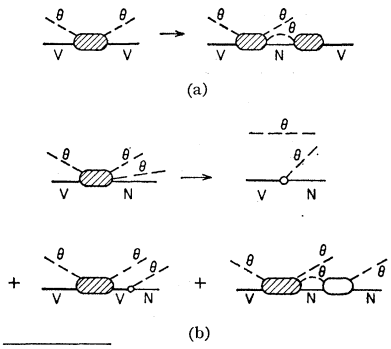

FIG. 1. (a) Dispersion graph for V–θ scattering corresponding to the division of the amplitude given in Eq. (2.6). (b) Dispersion graph for $F(\omega',\omega)$ as divided in Eq. (2.7). To each of the graphs there corresponds one more with θ particles interchanged.

[6] R. D. Amado, Phys. Rev. **122**, 696 (1961).
[7] T. D. Lee, Phys. Rev. **95**, 1329 (1954). M. L. Goldberger and S. B. Treimann, *ibid.* **113**, 1663 (1959).
[8] L. Castillejo, R. H. Dalitz, and F. J. Dyson, Phys. Rev. **101**, 453 (1956).
[9] The assumption of $m_V=m_n$ is in no way restrictive, and the case $m_V\neq m_n$ has been carried through.

Amado has solved the problem of $V\theta$ scattering in the standard Lee model exactly using dispersion theoretic methods. His method consists in solving the following equations, obtained by introducing intermediate states as shown in Fig. 1:

$$T(\omega)=\frac{2\Omega}{4\pi^2}\int_\mu^\infty \frac{k'u^2(\omega')F(\omega',\omega)K(\omega')}{\omega'}d\omega', \quad (2.6)$$

and

$$F(\omega',\omega)=-\frac{g\omega}{u^2(\omega)}\delta_{k,k'}+\frac{g}{2\Omega}T(\omega)\left(\frac{1}{\omega'}-\frac{1}{\omega'-\omega-i\epsilon}\right)+\frac{1}{\pi}\int_\mu^\infty \frac{k_1u^2(\omega_1)}{4\pi}M(\omega_1)F(\omega_1,\omega)\times\left(\frac{1}{\omega_1+\omega'-\omega-i\epsilon}+\frac{1}{\omega_1-\omega'+i\epsilon}\right)d\omega_1, \quad (2.7)$$

where

$$K(\omega)=[(2\omega\Omega)^{1/2}/u(\omega)]\langle 0|f(0)|N\theta_\omega{}^+\rangle,$$
$$T(\omega)=[(2\omega\Omega)^{1/2}/u(\omega)]\langle V|j(0)|V\theta_\omega{}^+\rangle, \quad (2.8)$$
$$F(\omega',\omega)=[(\omega\omega')^{1/2}/(u(\omega)u(\omega'))]\langle N\theta_{\omega'}{}^+|j(0)|N\theta_\omega{}^+\rangle, \quad (2.9)$$

and

$$f(t)=-i[d/dt]\psi_V(t),$$
$$j(t)=[(2\omega\Omega)^{1/2}/u(\omega)]\left(-i\frac{d}{dt}+\omega\right)\alpha_k(t). \quad (2.10)$$

ψ_V and α_k are destruction operators for V and θ particles, respectively, and Ω is the quantization volume. Equation (2.7) is an Omnes[10]-type integral equation in the variable ω, and can be easily solved. The polynomial-type ambiguity is absent in this case because of the convergence required in (2.6). The result obtained after these maniupulations is given by Amado which we quote

$$T(\omega)=-[g^2/\omega]/[1-\beta(\omega)-2/\{1+\omega\cdot C(\omega)\}], \quad (2.11)$$

where

$$C(\omega)=\frac{1}{\pi}\int_\mu^\infty \frac{\mathrm{Im}[1-\beta(\omega')]}{|1-\beta(\omega')|^2}\frac{1}{\omega'}\frac{\beta(\omega-\omega')}{1-\beta(\omega-\omega')}\frac{d\omega'}{\omega'-\omega}. \quad (2.12)$$

These results are directly applicable to our model also. As the stable V state and the $N\theta$ scattering states are in themselves complete,[11] the derivation of the integral equations is not affected by our modification. Also as only renormalized quantities are involved in (2.6) and (2.7), the solution is also unaffected by out modification. The effect of the modification is only felt via the function $1-\beta(\omega)$ appearing in (2.11) and (2.12).

[10] R. Omnes, Nuovo Cimento 8, 316 (1958).
[11] The author believes that this statement can be proved along the lines of reference 12.

Numerical Evaluation of the $V\theta$ Cross Section

We note that the integral (2.12) defining $C(\omega)$ does not have a singular integrand; although $(\omega'-\omega)$ does vanish at $\omega=\omega'$, the numerator $\beta(\omega-\omega')$, also vanishes at this point. Thus, the real and imaginary part of $C(\omega)$ can be evaluated without any difficulty. For a simple cutoff function $u^2(\omega)=\omega_0{}^2/[\omega^2-\omega_0{}^2]$ the function $1-\beta(\omega)$ can be evaluated in terms of elementary functions. The $V\theta$ cross section can then be determined using

$$e^{i\delta_{V\theta}(\omega)}\sin\delta_{V\theta}(\omega)=ku^2(\omega)T(\omega)/4\pi, \quad (2.13)$$

$$\sigma_{\mathrm{tot}}=\mathrm{Im}T(\omega)/k, \quad (2.14)$$

$$\sigma_{\mathrm{elas}}=|T(\omega)|^2/4\pi. \quad (2.15)$$

The results that we obtain in the Lee model would be physically sensible only if they are insensitive to the cutoff function. Thus, the parameters have to be chosen in a restricted range of values, so that the energies above the cutoff do not play an important role in any integral. It so happens that the real part of the function $1-\beta(\omega)$ has a minimum at some energy above the cutoff energy, and gives some unwanted bumps in the $N\theta$ cross sections if the V-$N\theta$ coupling constant is made very large. This fact also gives a large contribution to the function $C(\omega)$. In the numerical evaluation of $C(\omega)$, we restrict the parameters such that energies much higher than the cutoff had a small effect. This range of parameters is slightly more restrictive than that required for the elimination of the ghost V states. This still leaves a large scope of variations; especially the resonance in the $N\theta$ channel can be made as narrow as we like. In the results which are presented here the parameters were chosen so as to make $N\theta$ resonance appear like the 33 isobar. The mass of the resonance $\sim 1\mu$, the width $\sim 0.5\mu$, the C.D.D. zero was chosen at the threshold so that the $N\theta$ cross section behaved like a p-wave cross section. This, however, restricted our choice of V-$N\theta$ coupling constant to comparatively low values, $g^2/4\pi=0.3$. Figure 2(a) shows the $N\theta$ cross section that was used and Fig. 2(b) shows the $V\theta$ elastic and inelastic cross sections. We note the absence of any resonance of the type suggested by Peierls. Results of calculations with a side range of parameters confirm the above conclusion.

Analytic Properties of $C(\omega)$

The function $C(\omega)$, defined by the integral representation (2.12), has a logarithmic branch point at 2μ. The character of the function at this singularity can be easily studied by studying its imaginary part for

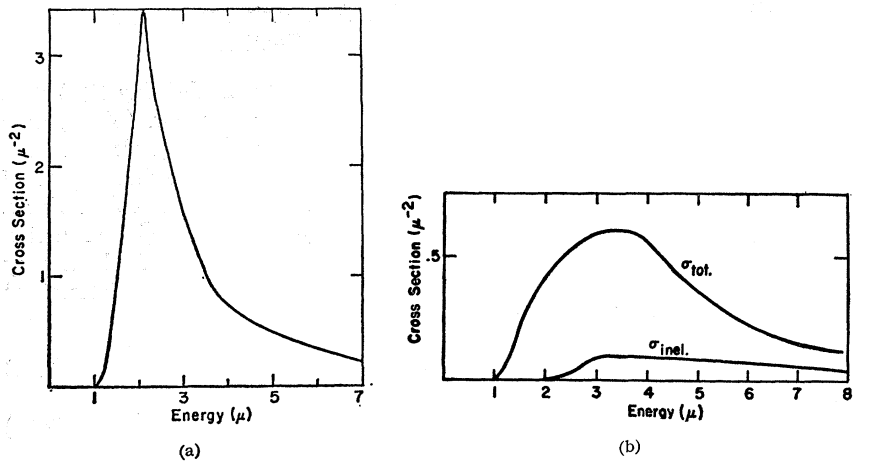

FIG. 2. (a) The $N\theta$ cross section which is used to calculate the $V\theta$ cross section in Fig. 2(b). The parameters are $g^2/4\pi=0.3$, $A=0.6$ and $\omega_0=1.0\mu$, and shows resonance around 2μ. (b) The $V\theta$ elastic and inelastic cross sections calculated with the $N\theta$ cross section in Fig. 2(a) as the input information.

$\mathrm{Im}\omega=+0$ and $\mathrm{Re}(\omega)$ slightly greater than 2μ.

$$\mathrm{Im}C(\omega)=-\frac{1}{\pi}\int_{\mu}^{\infty}\frac{\mathrm{Im}(1-\beta(\omega'))}{|1-\beta(\omega')|^2}\frac{1}{\omega'}\times\frac{\mathrm{Im}[1-\beta(\omega-\omega')]}{|1-\beta(\omega-\omega')|^2}\frac{d\omega'}{\omega'-\omega},\quad(2.16)$$

as $\mathrm{Im}\beta(\omega)=0$ for $\omega<\mu$, we can rewrite the above as

$$\mathrm{Im}C(\omega)=-\frac{1}{\pi}\int_{\mu}^{\omega-\mu}\frac{\mathrm{Im}(1-\beta(\omega'))}{|1-\beta(\omega')|^2}\frac{1}{\omega'}\times\frac{\mathrm{Im}[1-\beta(\omega-\omega')]}{|1-\beta(\omega-\omega')|^2}\frac{d\omega'}{\omega'-\omega}.\quad(2.17)$$

As in the entire range of integration in (2.17) the argument of $\beta(\omega)$ is near μ, we can treat every term except $k_\omega=(\omega^2-\mu^2)^{1/2}$ as a constant, thus,

$$\mathrm{Im}C(\omega)=\left[\frac{g^2}{4\pi}\frac{u^2(\mu)}{[1-\beta(\mu)]^2}\right]^2\frac{1}{4\mu}(\omega-2\mu)^2\quad\text{for}\quad\omega>2\mu.\quad(2.18)$$

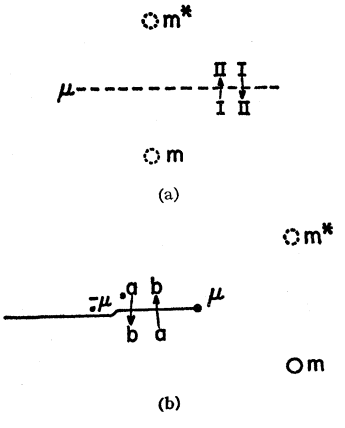

FIG. 3. (a) Connections between sheets I and II of the function $1/[1-\beta(\omega)]$. m and m^* are poles in the II sheet. (b) The figure shows the sheets a and b of the function $1/[1-\beta(\omega)]$, obtained from I and II, to be a clockwise rotation of the cut $\mu\to\infty$ to $-\infty\to\mu$. m is a pole in sheet a, and m^* in b. $-\mu$ is a branch point in sheet b.

Also

$$\mathrm{Im}C(\omega)=0,\quad\text{for}\quad\omega<2\mu,\quad(2.19)$$

from (2.18) and (2.19), it is obvious that the singularity of $C(\omega)$ at $\omega=2\mu$ has a logarithmic character.

$$C(\omega)=\text{const}-\left[\frac{g^2}{4\pi}\frac{u^2(\mu)}{[1-\beta(\mu)]^2}\right]^2\frac{1}{4\pi\mu}\times(\omega-2\mu)^2\ln(2\mu-\omega),\quad(2.20)$$

there is as indicated before no singularity for $\omega=\mu$.

As the analytic continuation of $C(\omega)$ involves analytic continuations of the function $1-\beta(\omega)$, we find it convenient at this point to discuss some of the properties of the latter.

It is apparent from the representation (2.5) that the function $1-\beta(\omega)$ has no singularities in the cut ω plane defined in Fig. 3(a).

$$1-\beta(\omega)=1-\frac{A\omega}{\omega-\omega_0}+\frac{g^2}{4\pi^2}\omega\int_{\mu}^{\infty}\frac{k'u^2(\omega')d\omega'}{\omega'^2(\omega'-\omega)}.\quad(2.21)$$

As ω crosses the real axis above μ from the upper half of the ω plane, we have to deform the contour and the resulting function has the representation

$$1-\beta^{\mathrm{II}}(\omega)=1-\beta(\omega)+i\frac{g^2}{2\pi}\frac{k(\omega)u^2(\omega)}{\omega}.\quad(2.22)$$

This cut is two sheeted due to the two-sheeted nature

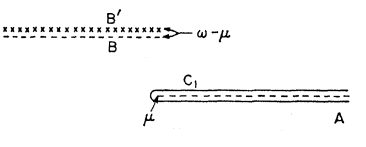

FIG. 4. The figure defines the contour C_1 in the ω plane. The branch lines A, B, and B' are defined in the text. The branch line B is in the same sheet as C_1, while B' is obtained by analytic continuation through A.

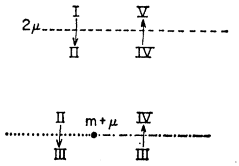

FIG. 5. The regions I–V in which $C(\omega)$ has different representations.

of $k(\omega)$. The function in the II sheet thus has all the singularities of $u^2(\omega)$, a pole at $\omega=0$ and a branch point at $\omega=-\mu$. More important, however, are the zeros of this expression which give rise to poles of $M(\omega)$ in the second sheet. For fairly large ω_0 these lie at complex conjugate points m and m^*, Fig. 3(a). Later, we have to rotate the cut to position $-\infty \rightarrow \omega+\mu$ when we find it convenient to define sheets a and b. As indicated in Fig. 3(b), $1-\beta^a(\omega)$ has a zero at m, and $1-\beta^b(\omega)$ at m^*.

Continuation of $C(\omega)$ to Higher Riemann Sheets

In order to obtain the continuation of the expression (2.12) for $C(\omega)$ to higher Riemann sheets, we rewrite it

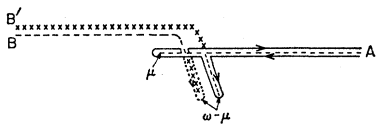

FIG. 6. The deformation of contour C_1 to obtain analytic continuation into region II. The dotted part of the contour in the sheet obtained by analytic continuation through A (hereafter called sheet II).

in the form of a contour integral

$$C(\omega)=-\frac{1}{2\pi i}\int_{C_1}\frac{1}{1-\beta(z)}\frac{dz}{z}\frac{\beta(\omega-z)}{1-\beta(\omega-z)}\frac{1}{z-\omega}, \quad (2.23)$$

where we have used the reality property $\beta^*(\omega)=\beta(\omega^*)$. The contour C_1 is defined in Fig. 4. The integrand is a function obtained by multiplying two functions having two sheeted cuts, and thus has four sheets. We call these cuts A for $[1-\beta(\omega)]^{-1}$ and B for $\beta(\omega-\zeta)$ $[1-\beta(\omega-\zeta)]$.

It should be noticed that the position of the cut B depends on ω and when we continue the function $C(\omega)$ as a function of ω, this may cross the contour of integration. In such cases we would have to deform the cut B and this would reveal the second-sheet singularities of the function $\beta(\omega)$. These in turn may cross the contour

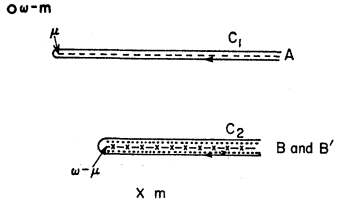

FIG. 7. This contour is obtained from that of Fig. 7 by rotating cut B clockwise.

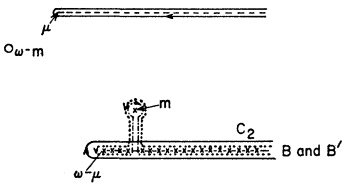

FIG. 8. Further deformation caused by the second-sheet pole of $[1-\beta(\omega)]^{-1}$. Notice that it affects the contour in the II sheet only.

of integration giving branch points in the second sheet of $C(\omega)$. We find it convenient to define five regions which are numbered I through V and are connected as shown in Fig. 5, in which the function $C(\omega)$ has different representations. These numbers do not denote the Riemann sheets of function.

As ω moves from region I to region II, the cut B crosses the contour in C_1, and to obtain an analytic continuation of $C(\omega)$, we have to deform the contour as shown in Fig. 6. Rotating cut B, we can reach the configuration shown in Fig. 7. The analytic representation of $C^{II}(\omega)$ can then easily be written

$$C^{II}(\omega)=-\frac{1}{2\pi i}\int_{C_1}\frac{1}{1-\beta(z)}\frac{dz}{z}\frac{\beta^a(\omega-z)}{1-\beta^a(\omega-z)}\frac{1}{z-\omega}$$
$$-\frac{1}{2\pi i}\int_{C_2}\left(\frac{1}{1-\beta(z)}-\frac{1}{1-\beta^{II}(z)}\right)$$
$$\times\frac{dz}{z}\frac{\beta^a(\omega-z)}{1-\beta^a(\omega-z)}\frac{1}{z-\omega}. \quad (2.24)$$

The deformations in the contour reveal two poles of the integrands; one at $z=m$ from the term $[1-\beta^{II}(z)]^{-1}$ and another at $z=\omega-m$ from the term $[1-\beta^a(\omega-z)]^{-1}$. These poles cause the region of validity of $C^{II}(\omega)$ to be limited, and as ω goes from II $\rightarrow$ III, we have to further deform the contours, as shown in Fig. 8. As the contours are deformed by a pole, it is easy to write the contribution

$$C^{III}(\omega)=C^{II}(\omega)-\frac{f^2}{m}\frac{1}{(m-\omega)}$$
$$\times\left[\frac{\beta^a(\omega-m)}{1-\beta^a(\omega-m)}-\frac{\beta^b(\omega-m)}{1-\beta^b(\omega-m)}\right], \quad (2.24a)$$

where f^2 is the residue of $[1-\beta^{II}(\omega)]^{-1}$ at $\omega=m$, and may be complex. Similarly when the pole at $z=\omega-m$ crosses C_1 (i.e., we go from region III–IV), we have to

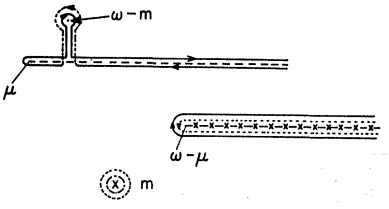

FIG. 9. Deformation of contour C_1 caused by pole of $[1-\beta^a(\omega-z)]^{-1}$.

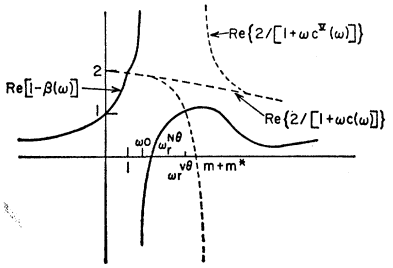

FIG. 10. Figure showing the energy dependence of $\mathrm{Re}[1-\beta(\omega)]$ and $\mathrm{Re}\{2/[1+\omega C(\omega)]\}$ in region I and V. It should be noticed that only the pole of $T(\omega)$ near $m+m^*$ is in the region V. There is, however, a pole below ω_0 in region I.

deform C_1 Fig. 9. and we get the continuation

$$C^{\mathrm{IV}}(\omega)=C^{\mathrm{III}}(\omega)-\frac{f^2}{m}\frac{1}{(\omega-m)}\times\left[\frac{1}{1-\beta^{\mathrm{II}}(\omega-m)}-\frac{1}{1-\beta^{\mathrm{I}}(\omega-m)}\right]. \quad (2.25)$$

Now when ω crosses real axis above 2μ in region IV–V, we get, as $C^{\mathrm{II}}(\omega)\rightarrow C^{\mathrm{I}}(\omega)=C(\omega)$,

$$C^{\mathrm{V}}(\omega)=C(\omega)-\frac{f^2}{m}\frac{1}{(m-\omega)}\left[\frac{\beta^a(\omega-m)}{1-\beta^a(\omega-m)}+\frac{1}{1-\beta^{\mathrm{I}}(\omega-m)}-\frac{\beta^b(\omega-m)}{1-\beta^b(\omega-m)}-\frac{1}{1-\beta^{\mathrm{II}}(\omega-m)}\right]. \quad (2.26)$$

The most important property of this function is that it has a pole at $\omega=m+m^*$ on the real axis (but not on the physical sheet), due to terms involving $1-\beta^{\mathrm{II}}(\omega-m)$ and $1-\beta^b(\omega-m)$. In the neighborhood of this point, we can represent $C^{\mathrm{V}}(\omega)$ by

$$C^{\mathrm{V}}(\omega)=-2\frac{f^2f^{2*}}{mm^*}\frac{1}{\omega-m-m^*}. \quad (2.27)$$

The analytic continuation of $C(\omega)$ also has poles at other points in these sheets; for example, it has a pole in region III at $\omega=2m$, where $\beta^a(\omega-m)/[1-\beta^a(\omega-m)]$ becomes infinite. Also left-hand singularities of $1-\beta^{\mathrm{II}}(\omega-m)$ contribute cuts at $m-\mu$ and there are poles far away due to $u^2(\omega)$, but none of these is very close to the overlap energy $\omega=m+m^*$.

Analytic behavior of $T(\omega)$. $T(\omega)$ is a function which is simply formed out of $1-\beta(\omega)$ and $C(\omega)$ Eq. (2.4), and has the cuts of both the functions. The analytic continuation of $T(\omega)$ to region V can be thus obtained simply by replacing $C(\omega)$ by $C^{\mathrm{V}}(\omega)$, $1-\beta(\omega)$ is unaffected as the path from region I–V takes it to the II sheet and back again to the I sheet.

$$T^{\mathrm{V}}(\omega)=-\frac{g^2}{\omega}\frac{1}{1-\beta(\omega)-2/[1+\omega\cdot C^{\mathrm{V}}(\omega)]}. \quad (2.28)$$

If we approximate $C^{\mathrm{V}}(\omega)$ by its pole term at $m+m^*$, it is easy to see (Fig. 10) that it causes the real part of the denominator in $T^{\mathrm{V}}(\omega)$ to vanish at an energy lower than $(m+m^*)$. As the residue at the pole of $C^{\mathrm{V}}(\omega)$ is negative, and the imaginary part of $1-\beta(\omega)$ is positive, the pole of $T^{\mathrm{V}}(\omega)$ would lie below the real axis. If the residue f^2 is very small, it is easy to see that this energy is very close to the energy $\omega=m+m^*$.

Thus, it appears that the pole conjectured by Peierls and by Tuan is present in the $V\theta$ scattering amplitude, but is not on a nearby sheet so as to contribute any bump to the physical cross sections.

3. THE MODIFIED LEE MODEL

We consider a system of heavy fermions V_1, V_2, and N, interacting with a light boson θ.[5] We choose V_1 and N to have the same mass which we also choose as zero of energy. The mass of V_2 is chosen as m, and that of θ particle as μ. All the fermions are taken as static, whereas θ obeys a relativistic energy-momentum relation. None of the particles has antiparticles, and the only allowed interactions are

$$V_1\rightleftarrows N+\theta,$$
$$V_2\rightleftarrows N+\theta. \quad (3.1)$$

First, we consider the situation in which V_2 is stable, and study the reactions

$$V_1+\theta\rightarrow V_1+\theta,$$
$$V_1+\theta\rightarrow V_2+\theta,$$

and

$$V_1+\theta\rightarrow N+\theta+\theta. \quad (3.2)$$

We denote the transition amplitudes for these reactions by $T_{11}(\omega)T_{22}(\omega)$ and $F(\omega',\omega)$, respectively, where ω is the total energy and ω', the energy of one of the θ particles in $N\theta\theta$ state. We also consider $V_2\theta$ elastic scattering with the amplitude $T_{22}(\omega)$.

The functions $T_{11}(\omega)$, $T_{12}(\omega)$ and $T_{22}(\omega)$ have cuts beginning with μ and $m+\mu$, which are two-sheeted, and a logarithmic cut beginning with 2μ arising from the three-particle state $N\theta\theta$. The continuation of the two-particle amplitudes through the two-particle channel has been discussed before[13] and we simply quote this:

$$T_{11}^{\mathrm{III}}(\omega)=\frac{T_{11}(\omega)(1+2i\rho_2(\omega)T_{22}(\omega))=2i\rho_2(\omega)T_{12}^2(\omega)}{(1+2i\rho_1(\omega)T_{11}(\omega))(1+2i\rho_2(\omega)T_{22}(\omega))+4\rho_1(\omega)\rho_2(\omega)T_{12}^2(\omega)}, \quad (3.3)$$

$$T_{12}^{\mathrm{III}}(\omega)=\frac{T_{12}(\omega)}{(1+2i\rho_1(\omega)T_{11}(\omega))(1+2i\rho_2(\omega)T_{22}(\omega))+4\rho_1(\omega)\rho_2(\omega)T_{12}^2(\omega)}, \quad (3.4)$$

[12] G. Kallen and W. Pauli, Kgl. Danske Videnskab. Selskab, Mat. Fys. Medd. **30**, No. 7 (1955).
[13] R. Oehme, Z. Physik **162**, 426 (1961).

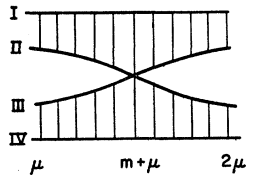

FIG. 11. The figure shows the connection between sheets I–IV connected along the real axis, as shown by vertical shading.

where $\rho_1(\omega)$ and $\rho_2(\omega)$ are phase-space factors for the $V_1\theta$ and $V_2\theta$ channels

$$\rho_1(\omega)=u^2(\omega)(\omega-m_1-\mu)^{1/2}, \quad \rho_2(\omega)=u^2(\omega)(\omega-m_2-\mu)^{1/2}.$$

The connection between the four sheets connected at μ and $m+\mu$ is shown in Fig. 11.

In general, the function $T_{22}(\omega)$ has a short cut in the physical sheet arising from the Born approximation graph Fig. 12. This shrinks to a pole in the static model. It is clear from (3.3) and (3.4) that the analytic continuations of $T_{11}(\omega)$ and $T_{12}(\omega)$ also have cuts at the same point, and these in our model will be poles. This is the singularity considered by Peierls and, hence, we are interested in studying its migration as V_2 becomes unstable.

In Appendix A we have studied the migration of the pole in the $N\theta$ scattering corresponding to V_2, as it becomes unstable. Applying the same results to the movement of the $V_2\theta$ branch points in the $V_1\theta$ scattering, we come to the conclusion that the branch point at $m+\mu$ in the physical sheet of $V_1\theta$ amplitude moves around the point 2μ as shown in Fig. 13, and takes the position $m^*+\mu$ in the upper half of the ω plane. At the same time, a branch point is found at $m+\mu$ in the lower half of the ω plane reached from the physical sheet by crossing the real axis, between 2μ and infinity from the upper half-plane. This branch point should correspond to the second sheet pole at m in the $N\theta$ scattering amplitude. When V_2 is stable, this should be the analog of the pole m' in the second sheet in $N\theta$ amplitude, as described in Appendix A. The cuts are shown in Fig. 13.

To illustrate the migration of the Peierls singularity, we consider the simplest perturbation theory graph in which it occurs, viz., Fig. 14. The matrix element of the graph is proportional to

$$\int_\mu^\infty \frac{k'u^2(\omega')d\omega'}{\omega'(\omega'-m_a)[\omega'-(\omega-m_b)]}, \tag{3.5}$$

which has as a function of ω a branch point at $m_b+\mu$, and in the sheet obtained by crossing this cut there are poles at $\omega=m_b$ and $\omega=m_a+m_b$. In the case where V_2 is stable, then clearly $m_a=m_b=m$, we have the well-known singularities already described. When the particle V_2 becomes unstable, we have to make m complex; however, we must have physical principles

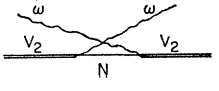

FIG. 12. Born approximation graph for $T_{22}(\omega)$.

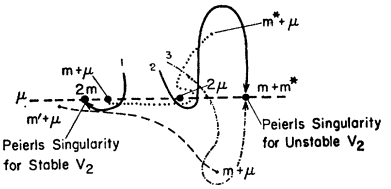

FIG. 13. The figure shows the various singularities of $V_1\theta \to V_1\theta$ scattering, for V_1 stable, and also for V_2 unstable. When V_2 is stable we have three cuts in the physical sheet, starting at μ, $m+\mu$, and 2μ, the thresholds for $V_1\theta$, $V_2\theta$, and $N\theta\theta$ channels, respectively. There is also a branch point in the second sheet at $m'+\mu$, where m' is the position of the second sheet pole in $N\theta$ scattering amplitude. There is a pole at $2m$ reached by path 1 from the physical sheet. This migrates as V_2 becomes unstable to $m+m^*$ reached along the path 2 from the physical sheet. There is, however, another pole reached by path 3, which has been discussed by Goebel, and also by us in Sec. 2 of this paper. This, however, cannot be easily connected to the case in which V_2 is stable, as long as we use perturbation theory, because the II sheet is not correctly described by a perturbation theory.

to choose the correct sheets. First, we require that the cuts move as shown in Fig. 14, and second, that the outgoing particles must be in decaying states. These conditions give $m_b=m^*$ and $m_a=m$. The Peierls singularity is then at $m+m^*$ reached as shown in Fig. 13.

4. CONCLUSION AND DISCUSSION

We have shown by an explicit calculation in the Lee model that the Peierls second resonance model is untenable once unitarity is correctly taken into account. Evidently, unitarity does not couple the $\pi N^* \to \pi N^*$ channel to the $\pi N \to \pi N$ channel as Peierls had conjectured. Although the present calculations were done in the Lee model, and crossing symmetry, recoil, etc., were ignored, we believe that they cast serious doubt on the validity of the Peierls mechanism. Probably the difficulty with the Peierls model arises from the treatment of the unstable particles on the same footing as the stable ones. In this connection we would like to draw the attention of the reader to the material in the Appendix A, where it is shown that the effect of a particle becoming unstable can not be taken into account simply by replacing m by $m-i\gamma$ where γ is positive and denotes the width of the resonance. This is because in most important cases, especially in the one under consideration, we do not want to make the particle stable by switching off the interaction, but by changing the mass conditions. This process involves an analytic continuation of the relevant functions as a function of the mass variable and in such cases the considerations in the Appendix A become relevant.

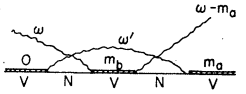

FIG. 14. Graph of lowest order having $V_2\theta$ scattering in the final state.

Lastly, we would like to point out that the amplitude for $V\theta$ scattering that we have used has a puzzling feature that it has a C.D.D. zero at precisely the same position as the C.D.D. zero in the $N\theta$ scattering amplitude. We are unable to account for this.

ACKNOWLEDGMENT

I am deeply indebted to Professor Dalitz for suggesting the problem, and for his help and criticism during the entire course of this work, without which it would have been impossible.

APPENDIX A

In this Appendix we follow the position of singularity representing a particle, as it becomes unstable.[14] In order to facilitate the discussion, we make the particle slightly unstable, and then we study the movement of the singularity as it becomes unstable with respect to the new channel. We illustrate this in the Lee model, which is described by the following Hamiltonian

$$H=m_V{}^0\psi_V{}^\dagger\psi_V+\sum_k\omega\alpha_k{}^\dagger\alpha_k+\sum_k w\beta_k{}^\dagger\beta_k + (g\psi_V{}^\dagger\psi_N A+\text{H.C.})+(f\psi_N{}^\dagger\psi_V\beta^\dagger+\text{H.C.}), \quad \text{(A1)}$$

where

$$\omega=(k^2+\mu^2)^{1/2}, \quad w=(k^2+\mu'^2)^{1/2}$$

$$A=\sum_k \frac{u(\omega)}{(2\omega r)^{1/2}}\alpha_k \quad \text{and} \quad B=\sum_k \frac{v(w)}{(2wr)^{1/2}}\beta_k, \quad \text{(A2)}$$

Ω is the quantization volume; later Ω is allowed to become infinite.

ψ_V and ψ_N are destruction operators for fermions V and N, and α_k and β_k are destruction operators of particles θ and θ' in momentum states k.[15] The mass of θ and θ' is μ and μ', respectively. The $N\theta$ scattering amplitude can now be simply written down

$$M(\omega)=\frac{g^2}{m_V{}^0-\omega-g^2\phi(\omega)-f^2\Phi(\omega)},$$

where

$$\phi(\omega)=\frac{1}{4\pi^2}\int_\mu^\infty \frac{k'u^2(\omega')d\omega'}{\omega'-\omega-i\epsilon}.$$

and

$$\Phi(\omega)=\frac{1}{4\pi^2}\int_\mu^\infty \frac{k'v^2(w')dw'}{w'-\omega-i\epsilon}, \quad \text{(A3)}$$

The physical V particle is then the pole of the function $M(\omega)$. This function has four sheets which can be numbered as shown in Fig. 15. The functions $\phi(\omega)$ and $\Phi(\omega)$ can be continued in the higher sheets

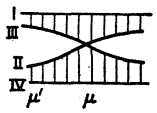

FIG. 15. The figure shows the connection between the sheets I–IV connected along the real axis, as shown by vertical shading. The function $M(\omega)$ has four sheets corresponding to two sheets each of $\phi(\omega)$, and $\Phi(\omega)$. The correspondence is as follows, I(1,1), II(2,2) III(1,2), and IV(2,1); where the two numbers in the paranthesis correspond to the sheets of the function $\phi(\omega)$and $\Phi(\omega)$, respectively.

very easily and we can then trace the path of the V-particle pole.[16] We take $\mu'<\mu$ and $f^2\ll g^2$, so that when Re $m_V<\mu$ there are two poles on the sheet III at complex conjugate positions. We show only the one reached from above the real axis, Fig. 16. There are also poles in the II sheet at points m_V' (lower than m_V). When $m_V{}^0$ is increased, these move as shown in Fig. 16 $m_V'\rightarrow m$ and $m_V\rightarrow m^*$. The pole m is in II sheet and m^* in IV sheet. As far as the poles $m_V{}^*$ and $m_V'{}^*$ are

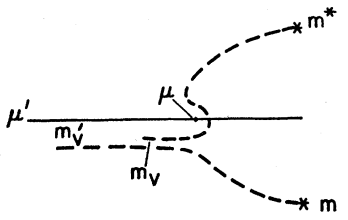

FIG. 16. Migration of the pole corresponding to V intermediate state in $N\theta$ scattering as it becomes unstable with respect to the $N\theta$ channel.

concerned, a similar trajectory takes them to m and m^* in IV and II sheets, respectively. We, thus, see that the poles which were close to the physical sheet are now on remote sheets and they are replaced by another pair, which was previously on remote sheets.

In the limiting case of $f^2=0$, the sheets I and III become identical, so do sheets II and IV. The V-particle singularities stay on the real axis till they meet on the II sheet and then they split apart into m and m^*.

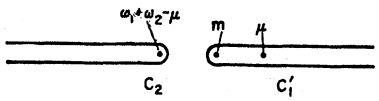

FIG. 17. Contour C_2 and C_1' in ω plane.

[14] G. Höhler, Z. Physik **152**, 546 (1958).

[15] The $N\theta'$ channel has been introduced only to make the V particle unstable even when below $N\theta$ threshold, so that it is never on the real axis. The pole can then be followed more easily. The coupling to the $N\theta'$ channel is thus necessarily vanishingly small. The above treatment is for s waves only.

[16] If we take a special cutoff function $u^2(\omega)=(\omega_0{}^2/\omega^2+\omega_0{}^2)$, the integral can be written down in terms of elementary functions.

$$\phi(\omega)=\frac{\mu^2\pi(\omega)}{\pi}\Big[-(\omega^2-\mu^2)^{1/2}\ln\Big[-\Big\{\omega+(\omega^2-\mu^2)^{1/2}\Big\}/\mu\Big] + \frac{\pi(\omega_0{}^2+\mu^2)^{1/2}}{2}+\frac{\omega}{\omega_0}(\omega_0{}^2+\mu^2)^{1/2}\sinh^{-1}(\omega_0{}^2+\mu^2)^{1/2}\Big],$$

where the sheets for the square root and logarithm functions have been chosen so that there is only one branch point, i.e., at $\omega=\mu$. This function is very simply obtained on the second sheet by adding the term $2i\pi(\omega^2-\mu^2)^{1/2}u^2(\omega)$. $\Phi(\omega)$ has also a similar representation. It is now a simple matter to trace the path of the V pole in (A2). The general nature of the trajectory is independent of the special choice of the cutoff function,

APPENDIX B

In this Appendix we discuss an extension of Amado's method[6] for $V\theta$ amplitude to the $N\theta\theta$ amplitude. As this extension is very direct, we omit the details, and present only the important steps. As we are interested, in this paper, in the three-particle states which have resonances in two pairs, we want to consider the V-particle as unstable. This, we find, leads to a solution for $N\theta\theta$ amplitude which has an ambiguity which can be resolved by introducing V as a stable particle and then analytically continuing to the case of unstable V. First, we treat the case of unstable V and point out the ambiguity, and then we give the form in which this ambiguity has been resolved. Consider the amplitude

$$F(\omega,\omega_1\omega_2)=\frac{(2\omega_1\Omega\cdot 2\omega_2\Omega\cdot 2\omega\Omega)^{1/2}}{u(\omega_1)u(\omega_2)u(\omega)}\langle N\theta^-|\,j\,|N\theta_1\theta_2^-\rangle, \quad \text{(B1)}$$

where

$$j(t)=\frac{(2\omega r)^{1/2}}{u(\omega)}\left(-i\frac{d}{dt}+\omega\right)\alpha_k(t), \quad \text{(B2)}$$

$\alpha_k(t)$ being the annihilation operator for the θ particle in momentum state k, $u(\omega)$ is the cutoff function introduced to cause convergence of all the relevant integrals, and Ω is the quantization volume later allowed to become infinite. The minus sign on the state indicates outgoing waves. This amplitude is the one which is required to take into account the effect of $N\theta\theta$ state as the final state.

First, we consider V in the continuum. Then the $N\theta$ states are complete and we can obtain a dispersion relation for this function in the variable by contracting the θ from the left in (B1)

$$\begin{aligned}F(\omega,\omega_1\omega_2)&=\frac{(2\omega\Omega)}{u^2(\omega)}\Big[\delta_{kk_1}\frac{(2\omega_2\Omega)^{1/2}}{u(\omega_2)}\langle N|\,j\,|N\theta_2^-\rangle\\&\quad+\delta_{kk_2}\frac{(2\omega_1\Omega)^{1/2}}{u(\omega_1)}\langle N|\,j\,|N\theta_1^-\rangle\Big]+\frac{(2\omega_1\Omega)^{1/2}}{u(\omega_1)}\frac{(2\omega_2\Omega)^{1/2}}{u(\omega_2)}\\&\quad\times\lim_{t\to\infty}\langle N|[\alpha_k(t),\,j]|N\theta_1\theta_2^-\rangle. \quad \text{(B3)}\end{aligned}$$

Introducing the intermediate states $|N\theta^-\rangle$ which are complete,[9] and using

$$M^*(\omega)=\frac{(2\omega\Omega)^{1/2}}{u(\omega)}\langle N|\,j\,|N\theta^-\rangle,$$

we get

$$\begin{aligned}F(\omega,\omega_1\omega_2)&=\frac{2\omega\Omega}{u^2(\omega)}[\delta_{k_1,k}M^*(\omega_2)+\delta_{k_2,k}M^*(\omega_1)]\\&\quad+\frac{1}{\pi}\int_\mu^\infty\frac{k'u^2(\omega')}{4\pi}M^*(\omega')F(\omega',\omega_1\omega_2)\\&\quad\times\left[\frac{1}{\omega'-\omega-i\epsilon}+\frac{1}{\omega'-(\omega_1+\omega_2-\omega)+i\epsilon}\right]d\omega'. \quad \text{(B4)}\end{aligned}$$

This is an Omnes[10] type equation which can be easily solved; however, it is easy to see that the inhomogeneous term itself is a solution of the equation. If we substitute

$$[2\omega\Omega/u^2(\omega)]\delta_{k_1,k}M^*(\omega_2)$$

in the integral, we get

$$M^*(\omega_1)M^*(\omega_2)\left[\frac{1}{\omega_2-\omega-i\epsilon}-\frac{1}{\omega_1-\omega+i\epsilon}\right]. \quad \text{(B5)}$$

This is odd under the exchange $1\rightleftarrows 2$. Thus, the sum of this term and the term for $[2\omega\Omega/u^2(\omega)]\delta_{k_2,k}M^*(\omega_1)$ vanishes. Thus, this inhomogeneous term, plus a solution of the homogeneous equation, gives the complete solution. We can prove that

$$M(\omega)M^*(\omega_1+\omega_2-\omega)$$

is a solution of the homogeneous equation in the case where $M(\omega)$ has no poles in the physical sheet, as follows: Consider the integral

$$\begin{aligned}I=-\frac{1}{\pi}\int_\mu^\infty&\frac{k'u^2(\omega')}{4\pi}|M(\omega')|^2M^*(\omega_1+\omega_2-\omega')\\&\times\left[\frac{1}{\omega'-\omega-i\epsilon}+\frac{1}{\omega'-(\omega_1+\omega_2-\omega)+i\epsilon}\right]d\omega'. \quad \text{(B6)}\end{aligned}$$

This can be rewritten as a contour integral,

$$\begin{aligned}I=\frac{1}{2\pi i}\int_{C_1}&M(\omega')M^*(\omega_1+\omega_2-\omega')\\&\times\left[\frac{1}{\omega'-\omega-i\epsilon}+\frac{1}{\omega'-(\omega_1+\omega_2-\omega)+i\epsilon}\right]d\omega', \quad \text{(B7)}\end{aligned}$$

which can be easily integrated

$$\begin{aligned}I=-\frac{1}{2\pi i}\int_{C_2}&M(\omega')M^*(\omega_1+\omega_2-\omega')\\&\times\left[\frac{1}{\omega'-\omega-i\epsilon}+\frac{1}{\omega'-(\omega_1+\omega_2-\omega)+i\epsilon}\right]d\omega'\\&+2M(\omega)M^*(\omega_1+\omega_2-\omega). \quad \text{(B8)}\end{aligned}$$

The integral on the right-hand side of this equation is seen to be equal to I when we make a change in the integration variable $[\omega'\to(\omega_1+\omega_2-\omega')]$. Thus, a solution of (B4) is

$$\begin{aligned}F(\omega,\omega_1\omega_2)&=\frac{2\omega\Omega}{u^2(\omega)}(\delta_{k_1,k}M(\omega_2)+\delta_{k_2,k}M(\omega_1))\\&\quad+A(\omega_1,\omega_2)M(\omega)M^*(\omega_1+\omega_2-\omega). \quad \text{(B9)}\end{aligned}$$

The coefficient $A(\omega_1,\omega_2)$ is not determined by the integral equation we have solved. This should not be surprising as there are many Lee models, with different

numbers of V in the $N\theta$ continuum which leads to the same equation. The coefficient $A(\omega_1,\omega_2)$ may be determined by analytical continuation from the case of stable V particles. The more complete equations are

$$F(\omega,\omega_1\omega_2)=\frac{2\omega\Omega}{u^2(\omega)}[\delta_{k,k_1}M^*(\omega_2)+\delta_{k_2,k}M^*(\omega_1)]$$
$$-gT(\omega_1,\omega_2)\left[\frac{1}{m-\omega}+\frac{1}{m-(\omega_1+\omega_2-\omega)}\right]$$
$$+\frac{1}{\pi}\int_\mu^\infty e^{-i\delta(\omega')}\sin\delta(\omega')F(\omega',\omega_1\omega_2)$$
$$\times\left[\frac{1}{\omega'-\omega-i\epsilon}+\frac{1}{\omega'-(\omega_1+\omega_2-\omega)+i\epsilon}\right]d\omega', \quad \text{(B10)}$$

and

$$T(\omega_1,\omega_2)=\sum_{\omega'}\frac{K^*(\omega')u^2(\omega')}{(2\omega'\Omega)}\frac{F(\omega',\omega_1\omega_2)}{(\omega'-i\epsilon)}, \quad \text{(B11)}$$

where

$$T(\omega_1,\omega_2)=\frac{(2\omega_1\Omega\cdot 2\omega_2\Omega)^{1/2}}{u(\omega_1)u(\omega_2)}\langle V|j|N\theta_1\theta_2^-\rangle, \quad \text{(B12)}$$

and

$$K^*(\omega)=\frac{(2\omega\Omega)^{1/2}}{u(\omega)}\langle 0|f|N\theta_\omega^-\rangle. \quad \text{(B13)}$$

These are soluble exactly by the method used by Amado. We put the result in a slightly different form

$$F(\omega,\omega_1\omega_2)=\frac{2\omega\Omega}{u^2(\omega)}[M^*(\omega_1)\delta_{k,k_2}+M^*(\omega_2)\delta_{k,k_1}]+\frac{2M^*(\omega_1)M^*(\omega_2)M(\omega)M^*(\omega_1+\omega_2-\omega)}{g^2M^*(\omega_1+\omega_2-\omega)+\frac{1}{4\pi^2}\int_\mu^\infty ku^2(\omega)|M(\omega')|^2M(\omega_1+\omega_2-\omega')d\omega'}. \quad \text{(B14)}$$

The denominator in (B14) can be easily put in the form of a contour intetral

$$D(\omega_1+\omega_2)=g^2M^*(\omega_1+\omega_2-m)$$
$$+\frac{1}{2\pi i}\int_{C_1}M(\omega)M^*(\omega_1+\omega_2-\omega)d\omega, \quad \text{(B15)}$$

where D is the denominator function in (B14). Here we see that the first term is just the residue of the integrand at the point $\omega=m$. Thus, we can easily define a new contour C_1' to go around m when, leading to the expression

$$D(\omega_1+\omega_2)=\frac{1}{2\pi i}\int_{C_1'}M(\omega)M^*(\omega_1+\omega_2-\omega)d\omega. \quad \text{(B16)}$$

This result holds whether or not V is stable because all that happens is that the V-particle pole in $M(\omega)$ migrates to the II sheet of the function. As C_1' already encloses this pole, no singularity crosses any contour of integration. Hence, for a stable V particle, we have

$$A(\omega_1,\omega_2)=2M^*(\omega_1)M^*(\omega_2)\Big/\frac{1}{2\pi i}\int_{C_1'}M(\omega)$$
$$\times M^*(\omega_1+\omega_2-\omega)d\omega, \quad \text{(B17)}$$

and the expression remains valid when the V particle lies in the continuum. The function $D(\omega)$ has properties quite similar to those of $C(\omega)$; in particular it has a pole in region V. This may give rise to a zero of $D(\omega)$ close to $\omega=m+m^*$, which might show up as a bump in $A^V(\omega_1,\omega_2)$; however, this is not physically interesting.